

Simulation Standard

TCAD Driven CAD

A Journal for Process and Device Engineers

Simulating Boron Diffusion in Silicon Germanium

Introduction

The silicon germanium heterojunction bipolar transistor (SiGe HBT) is a promising technology for combining the operating speed of compound material devices with the production capability of bulk silicon. The presence of a narrower-bandgap material in the base region where most of the bandgap offset occurs in the valence band, creates an energy well for holes. With the lower energy barrier, a lower hole current density can be obtained for a given electron current density increasing the transistor's gain [1]. Thus the base can then be highly doped, greatly increasing high frequency performance whilst still retaining a reasonable gain. For this reason, the diffusion of boron in SiGe is of great interest.

The incorporation of high boron levels in the base region along with the Ge-induced effects makes prediction of boron diffusion through the SiGe layer difficult. Published experimental data has shown that boron diffusion in SiGe differs from that in bulk silicon. Specifically, experimental evidence indicates that the boron diffusivity in SiGe is dependent on the concentration of germanium with boron diffusivity decreasing as the germanium content increases [2, 3]. To account for such effects, a diffusion model has been implemented in *SSuprem4* for the diffusion of boron in SiGe.

Boron Diffusion in SiGe

In the new diffusion model, silicon germanium is treated as highly-Ge-doped silicon. The model takes into account two effects discussed in published works: 1) boron diffusivity decreases exponentially with Ge content [2] and 2) intrinsic carrier concentration increases linearly with Ge content [3]. Strain effects are considered negligible in this model. To account for the exponential variation of boron diffusivity with Ge content, the boron diffusivity term associated with the neutral boron-interstitial pair is modeled as:

$$D_{BI}^x = DIX.0 \exp\left(-\frac{DIX.E + x \cdot EAFAC.T.SIGE}{kT}\right) \quad (1)$$

where *DIX.0* and *DIX.E* are the prefactor and activation energy for the diffusivity of a neutral boron-interstitial pair in silicon, *x* is the Ge fraction of the SiGe layer, *k* is the Boltzman constant, *T* is temperature, and *EAFAC.T.SIGE* is a calibration parameter. Similarly, the linear variation of intrinsic carrier concentration with Ge content is modeled as:

$$n_i^{SiGe} = n_i^{Si} \cdot (1 + x \cdot NIFAC.T.SIGE) \quad (2)$$

where *NIFAC.T.SIGE* is a calibration parameter and n_i^{Si} is the intrinsic carrier concentration of silicon calculated as:

$$n_i^{Si} = NI.0 \exp\left(-\frac{NI.E}{kT}\right) \cdot T^{NI.POW} \quad (3)$$

where *NI.0*, *NI.E*, and *NI.POW* are additional calibration parameters. The user-defined calibration parameters *EAFAC.T.SIGE* and *NIFAC.T.SIGE* have default values of 1.5 and 100, respectively. The value of these calibration parameters as well as the value of *NI.0*, *NI.E*, or *NI.POW* can be set on the *MATERIAL* statement. The diffusion model for boron diffusion in silicon germanium

Continued on page 2....

INSIDE

Simulating 3D OHMIC Heating Effects in Metal	5
The Valdinoci Temperature Dependent Impact Ionization Model for Silicon	7
Calendar of Events	10
Hints, Tips, and Solutions	11

is activated with the *MODEL.SIGE* parameter on the *METHOD* statement.

Because SiGe layers are treated as Ge-doped silicon in the new diffusion model, adding SiGe layers to existing *ATHENA* structures is handled a little differently. Silicon germanium layers are added to a structure using the *DEPOSIT* statement, however they are added as silicon rather than SiGe. The Ge concentration in the deposited layer is set using the *C.GERMANIUM* parameter and should be calculated as:

$$C.GERMANIUM = x \cdot N_{si} \quad (4)$$

where N_{si} is the atomic density of undoped silicon (5×10^{22} atoms/cm³). Specifying a germanium concentration in the above manner will create a SiGe layer with uniform Ge content. To create a layer with a graded composition profile, a second parameter, *GE.FINAL*, must be specified on the *DEPOSIT* statement. When *GE.FINAL* is used, *C.GERMANIUM* specifies the initial germanium concentration and *GE.FINAL* specifies the final germanium concentration. For example, the following *DEPOSIT* statement defines a 0.1 micron thick SiGe layer with a graded Ge profile starting at $x = 0.002$ at the lower boundary and increasing linearly to $x = 0.2$ at the upper boundary:

```
DEPOSIT SILICON THICK=0.1 DIV=10 \
C.GERMANIUM=1E20 GE.FINAL=1E22
```

With the new diffusion model, *ATHENA* treats SiGe as Ge-doped silicon. This however is not the case for *ATLAS*. Before exporting a structure to the device simulator, Ge-doped silicon regions must be converted to silicon germanium. To convert those regions include the *SIGE.CONV* parameter on the *STRUCTURE* statement. When the *SIGE.CONV* parameter is specified, all silicon material nodes with a germanium concentration above 5×10^{19} cm⁻³ are converted to silicon germanium material nodes. The composition fraction at the converted nodes is calculated as:

$$x = \frac{C_{Ge}}{N_{Si}} \quad (5)$$

Simultaneously, all Ge, active Ge, and donor or acceptor concentrations associated with the Ge content are removed from the structure. This conversion only works for 2D structures.

Simulation Results

To evaluate the general performance of the new model for boron diffusion in silicon germanium, a test structure similar to that proposed by R. Lever *et al.* [3] was created using *SSuprem4*. The structure consists of a uniformly-doped silicon epilayer sandwiched between two thin layers of SiGe. Beneath the SiGe/Si/SiGe stack is a 10 micron silicon substrate. Above the SiGe/Si/SiGe stack

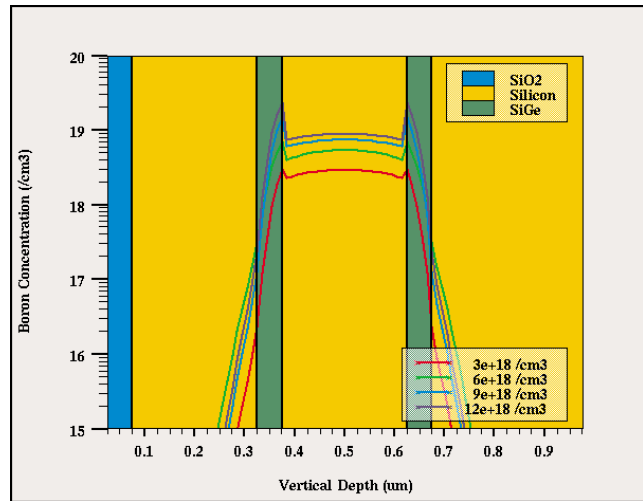


Figure 1. Comparison of boron profiles for varying initial doping concentrations; structure annealed for 12 hours at 850°C; uniform Ge fraction of 10%.

is a 0.25 micron silicon layer and a 0.25 micron oxide cap. The base doping level of the silicon epilayer was 6×10^{18} cm⁻³. The SiGe layers were initially given a uniform composition fraction of 10%. The Fully-Coupled diffusion model was used for all of the simulations.

The most outstanding feature of the simulation results is the pileup of boron at the Si/SiGe interface. As reported by R. Lever *et al.* [3], this occurs because boron has a higher activation energy in silicon than in silicon germanium. Figure 1 shows the boron profiles following a 12 hour, 850°C anneal for initial doping concentrations of 3×10^{18} cm⁻³, 6×10^{18} cm⁻³, 9×10^{18} cm⁻³, and 12×10^{18} cm⁻³. As can be seen, the boron pileup increases with concentration, and the boron diffusivity in SiGe is significantly lower than it is in silicon. The results also show that the doping dependence of the boron pileup begins to saturate for concentrations above 1×10^{19} cm⁻³.

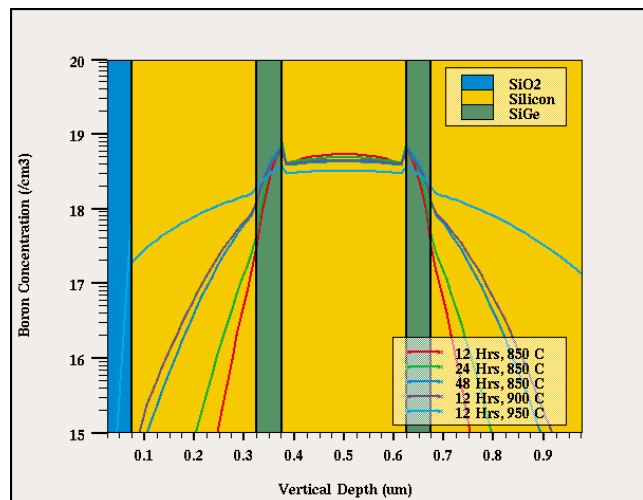


Figure 2. Comparison of boron profiles for varying diffusion conditions; initial boron concentration of 6×10^{18} cm⁻³; uniform Ge fraction of 10%

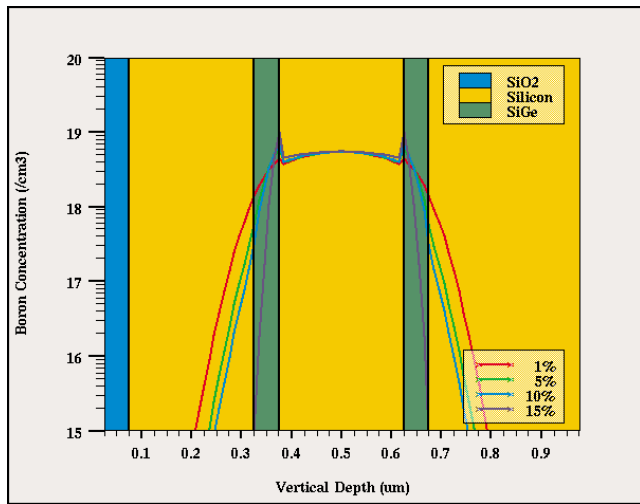


Figure 3. Comparison of boron profiles for varying Ge composition fractions; initial boron concentration of $6 \times 10^{18} \text{ cm}^{-3}$; structure annealed for 12 hours at 850°C .

Boron diffusion in SiGe behaves similarly to that in silicon for varying diffusion times and temperatures. Figure 2 shows the boron profiles following diffusions of 12, 24, 36, and 48 hours at 850, 900, and 950°C . Again it can be seen that the boron pileup is dependent on the initial boron concentration. It is not dependent on the initial diffusion conditions. As expected, the boron profile extends further out from the central silicon epilayer as either the diffusion time or temperature is increased. Figure 3 shows the boron profiles for a Ge content of 1, 5, 10, and 15%. Both boron pileup and diffusivity are significantly affected by the Ge content. At 1%, the resulting boron profile shows very little pileup and essentially no reduction in diffusivity. However at 15%, significant pileup occurs and the diffusivity is low enough that little boron diffuses through the SiGe boundary layers. As will be shown, the influence of Ge content on the diffusion behavior of boron over such a narrow content range can have profound effects on the boron profile in graded SiGe regions.

Most practical devices do not use uniform germanium content in the base, as this results in impractically thin base region before strain related defects occur. To reduce strain and increase base width, most devices have base regions with “graded” germanium profiles. It is important therefore to examine how well the new diffusion model handles graded profiles. Figure 4 shows the boron profiles from three separate test structures. The first structure included SiGe boundary layers with a graded Ge profile. The Ge content of the graded SiGe regions varied linearly from 10% at the outside edge of the SiGe boundary region to 1% at the inside edge. The second structure includes SiGe boundary layers with uniform Ge content of 10%. In the final

structure, the SiGe boundary layers were replaced with undoped silicon. The central silicon epilayer for all three structures was initially doped at $6 \times 10^{18} \text{ cm}^{-3}$. All three structures were annealed at 850°C for 12 hours in an inert ambient.

The boron profile for the structure with the uniform SiGe regions is very similar to those profiles presented in Figures 1-3. A moderate amount of boron pileup is observed at the Si/SiGe interface and the diffusivity of boron is noticeably reduced within the SiGe boundary layers. The boron profile in the graded structure differs significantly. Very little pileup is seen at the SiGe interface due to the low Ge content at that boundary. The boron diffusivity at the inner Si/SiGe interface is close to that in the silicon structure. It decreases across the graded SiGe layer reaching a minimum at the outer interface. As can be seen from these results, properly modeling boron diffusion across the SiGe base region of a HBT device is key when simulating technologies with graded base regions. If the device designer were to assume a uniform Ge profile or silicon-like diffusion properties, the simulated junction depth would be significantly different than that of the actual device.

As with any simulation, some level of model calibration is generally needed to match experimental results. To this end, the new diffusion model for boron in SiGe provides two calibration parameters: *EAFACT.SIGE*

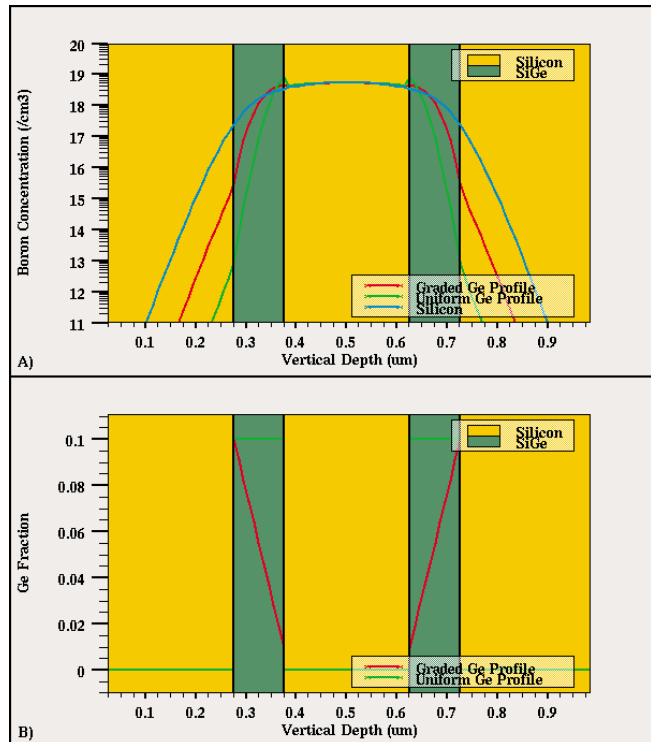


Figure 4. A) Boron profiles for graded Ge-profile structure, uniform Ge-profile structure, and silicon structure. B) Ge profiles for graded and uniform structures.

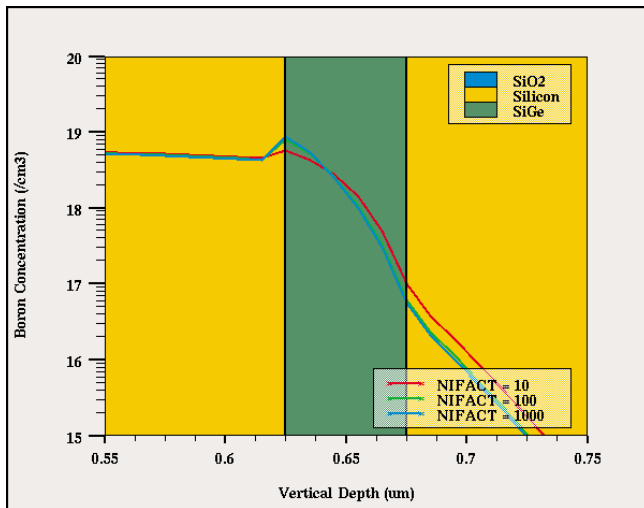


Figure 5. Comparison of boron profiles for varying values of *NIFACT.SIGE*; initial boron concentration of $6 \times 10^{18} \text{ cm}^{-3}$; structure annealed for 12 hours at 850°C .

and *NIFACT.SIGE*. Figures 5 and 6 show the boron profiles for differing values of *NIFACT.SIGE* and *EFACT.SIGE*, respectively. For both sets of simulations, the initial boron concentration in the central silicon epilayer is $6 \times 10^{18} \text{ cm}^{-3}$. The structures were annealed at 850°C for 12 hours in an inert ambient. Variations in *NIFACT.SIGE* directly affect the amount of boron pileup at the Si/SiGe interface. Variations in *NIFACT.SIGE* do not significantly affect boron diffusivity in the SiGe layers. It should also be noted that a significant deviation from the default value was necessary to see any significant change in the profile. The performance of the new diffusion model for boron in SiGe does not appear to be sensitive to variations in *NIFACT.SIGE* under these conditions. The new diffusion model was much more sensitive to variations in *EFACT.SIGE*. The value of *EFACT.SIGE* does not appear to alter the amount of pileup at the Si/SiGe interface much, but it has a significant affect on the amount of diffusivity reduction in the SiGe regions. This is expected due to the nature of Equation 1.

Summary

Following the work of [2] and [3], a new model for the diffusion of boron in silicon germanium has been implemented in *SSuprem4*. This new diffusion model treats SiGe as highly-Ge-doped silicon and accounts for two effects: 1) boron diffusivity decreases exponentially as the Ge content increases and 2) the intrinsic carrier concentration increases linearly as the Ge content increases. To evaluate the general behavior of the new model, a simple test structure was created with which various doping and diffusion conditions were studied.

The most outstanding feature of the new model is the resulting boron pileup at the Si/SiGe interface. It was also shown that the diffused profiles in layers with uniform and graded Ge profiles differ significantly.

References

- [1] D. Vook et al., "Double-Diffused Graded SiGe Base Bipolar Transistors," *IEEE Transactions on Electron Devices*, vol. 41, pp. 1013-1018, June 1994.
- [2] K. Rajendran et al., "Simulation of Boron Diffusion in Strained Si_{1-x}Ge_x Epitaxial Layers," *SYSPAD-2000*, pp. 206-209.
- [3] R. Lever et al., "Boron Diffusion Across Silicon-Silicon Germanium Boundaries," *Journal of Applied Physics*, vol. 83, pp. 1988-1994, February 15, 1998.

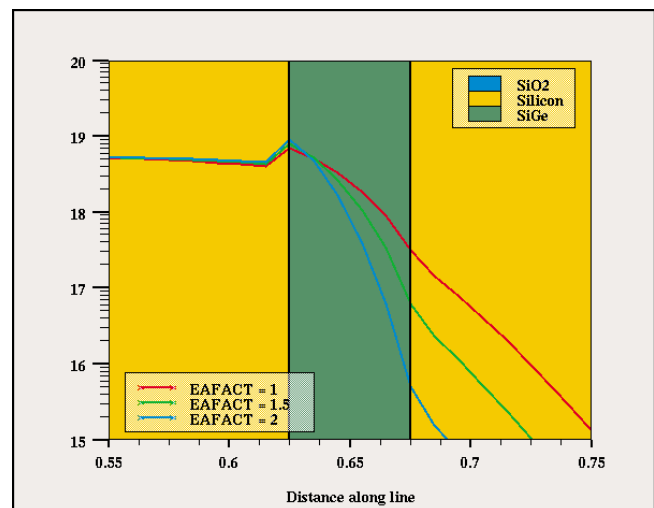


Figure 6. Comparison of boron profiles for varying values of *EFACT.SIGE*; initial boron concentration of $6 \times 10^{18} \text{ cm}^{-3}$; structure annealed for 12 hours at 850°C .

Simulating 3D OHMIC Heating Effects in Metal

Introduction

A new feature has been added to Silvaco's device simulator *ATLAS*, which allows the simulation of ohmic heating effects in metals using the *Giga* or *Giga3D* modules. The feature has been included in response to metal heating problems that increasingly occur in interconnects for very aggressive technologies.

Normally metals in device simulators are treated as either ohmic or Schottky contacts with little regard for their bulk resistivity, since this is usually insignificant compared to the resistivity of the underlying semiconductor.

The new feature now allows the ohmic resistance, and the heating it causes, to be taken into account for both 2D and 3D arbitrary device structures. The steady state simulations allow temperature dependent thermal resistivities and conductivities to be defined by the user, so any arbitrary metal could be defined.

Heating effects can also be investigated in time domain by applying a transient pulse to the structure. For such simulations, the temperature dependent specific heat capacities for the materials can also be defined by the user.

The simulation of ohmic resistance in a metal is activated using the new key word "conductor" on the region statement containing the metal. For example, the following region statement defines a 10um long aluminum interconnect that is 0.5um wide and 0.6um thick:

```
region number=1 material=Aluminum \  
conductor x.min=0 x.max=0.5 \  
y.min=0 y.max=0.6 z.min=0 z.max=10
```

The temperature dependent resistivity coefficient can be specified using the "drhodt" parameter in the material statement. An example is shown below:

```
material material=Aluminum drhodt=0.00429
```

Thermal resistivity coefficients for a number of known metals have been included as default parameters. These values were taken from reference 1.

Aside from these two new parameters, all aspects of simulating self heating effects using *Giga* and *Giga3D* remain as before, so the user may reference the manual and the many *DeckBuild* examples for further information.

Steady State Example

A simple "dogbone" type structure was constructed using the *ATLAS Device3D* simulator. One electrical contact was defined at each end of the dogbone and these contacts were held at 300K (room temperature).

In order to simulate radiation from the top of the device through the surrounding oxide to the air, a thermal contact was defined covering the entire top surface and a further thermal contact was defined on the bottom of the structure to simulate conduction through to the substrate.

The resulting structure in Figure 1 shows a *TonyPlot3D* image of the surface and side temperature contours of the surrounding oxide following the application of a suitable voltage across the two contacts. Figure 2 shows the same structure but with the surrounding oxide hidden, a standard features of *TonyPlot3D*, so that the temperature contours of the aluminum conductor can be seen.

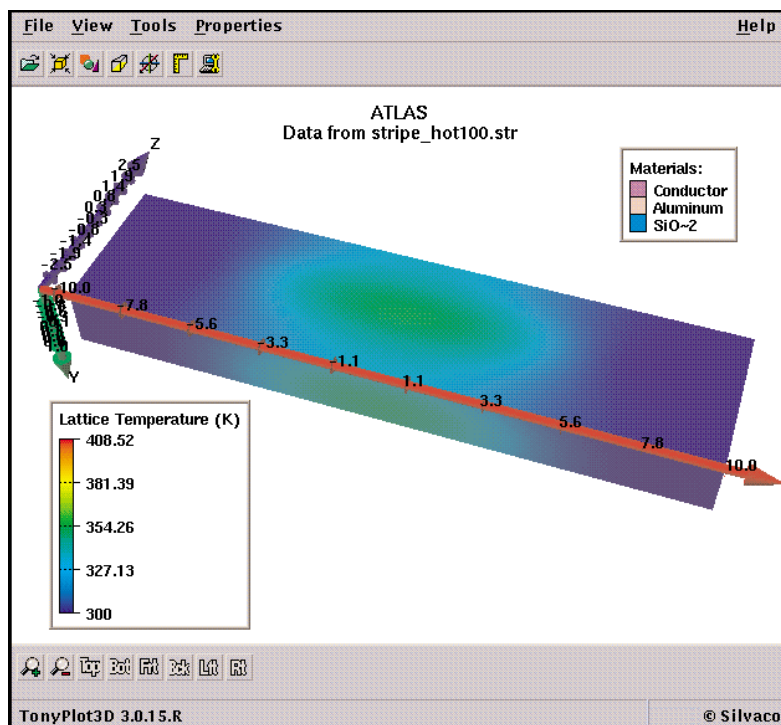


Figure 1. Temperature plot at the surface of the passivation oxide due to thermal heating of a buried interconnect aluminum line.

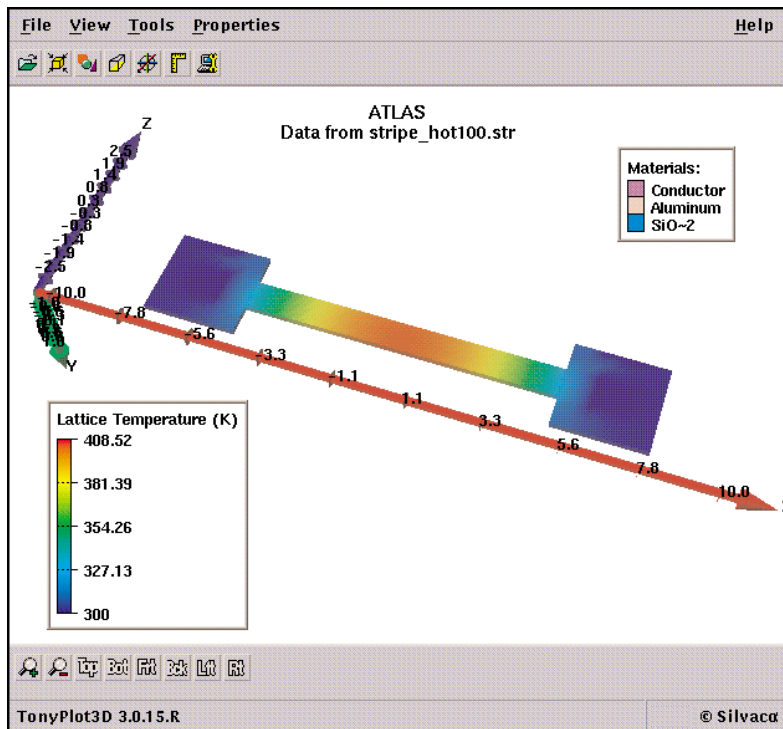


Figure 2. The same plot as Figure 1, but with the underlying conductor revealed with the *TonyPlot3D* "hide" feature.

Transient Example

In this example, the same structure was used, but instead of applying a steady state voltage across the conductor to dissipate power, a voltage pulse with a rise time of 1ns was applied for 10us, then turned off again at the same ramp rate. The relevant solve statements are reproduced below:

```
solve vanode=0.1 endramp=1e-9 \
tstop=1e-5 dt=1e-11
```

```
solve vanode=0 endramp=1e-9 \
tstop=2e-5 dt=1e-11
```

Thermal specific heat capacities are defined using the material statement in the normal way. Several temperature dependent models are available to the user. The resulting temperature rise waveform from what was effectively a square wave voltage pulse is shown in Figure 3, giving the expected result.

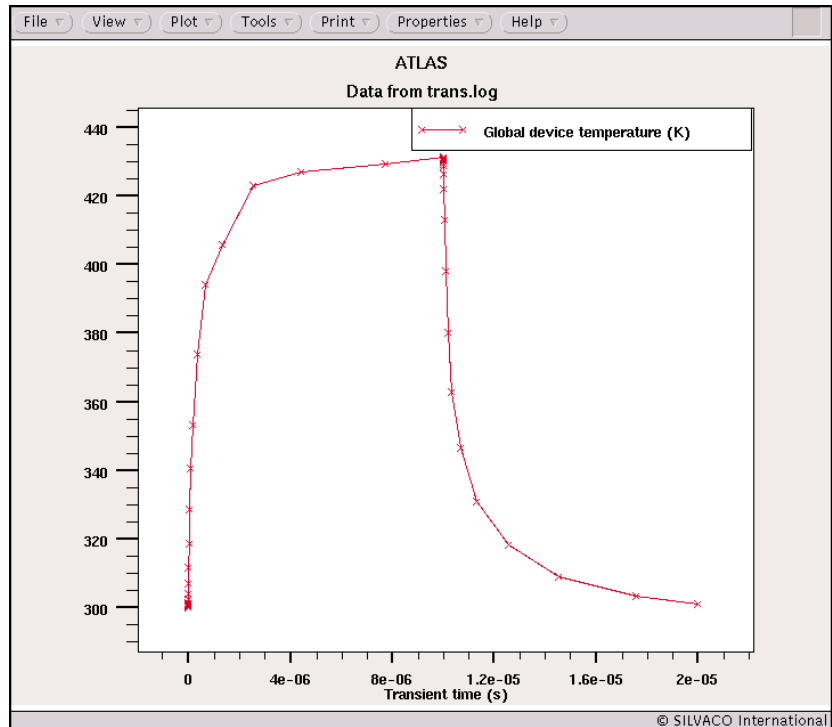


Figure 3. Transient heating at the center of a metal line as a result of a square waved voltage pulse applied to it's end.

Conclusion

A new *ATLAS Giga* and *Giga3D* capability has been demonstrated and examples given as to a typical use. The new capability will be available to existing customers who have the *Giga* or *Giga3D* modules as no new module will be required. If you are interested in this new feature and currently do not have a *Giga* or *Giga3D* license, please contact your account manager for further details.

References

- [1] Handbook of Chemistry and Physics, 56th Edition, 1975-76, CRC Press.

The Valdinoci Temperature Dependent Impact Ionization Model for Silicon

Impact ionization plays an important role in the design of many semiconductor devices. Since impact ionization is both temperature and electric field dependent, it is important to use a model which has the correct functional behavior. For most devices impact ionization defines the safe region of operation within a moderate range of temperatures, so the temperature dependence of impact ionization is of lesser importance than the field dependence. However, for devices which must operate outside of the usual temperature limits, or which carry enough current to heat themselves out of those limits, both field dependence and temperature dependence of the model must be accurate.

Impact ionization has been measured and modeled extensively at room temperature. Recently, Valdinoci et al.[1], have extended the measured temperature range to 400oC and developed a compact model for both electron and hole impact ionization. Their analytic model is given by

$$\alpha_{n,p} = E / (a(T) + B(T) \exp[d(T)/(E + c(T))])$$

where E is the electric field along the current flow lines. The parameters a (), b (), c () and d () are defined according to:

$$a(T) = a_0 + a_1 * T^{a_2}$$

$$b(T) = b_0 * \exp[b_1 * T]$$

$$c(T) = c_0 + c_1 * T^{c_2} + c_3 * T^2$$

$$d(T) = d_0 + d_1 * T + d_2 * T^2$$

This model is now available in *ATLAS*. It is enabled by specifying VALDINOCI on the IMPACT statement. Valdinoci's fitted parameters for silicon are the default and are shown in Table 1. The model parameters for electrons and holes can be modified by specifying the parameters VALAN0, VALAP0, etc., on the IMPACT statement.

In contrast to Valdinoci's model, the Selberherr impact ionization model is simpler:

$$\alpha = A(T) \exp[-(B(T)/E)^{\beta}]$$

where the parameters A and B are temperature dependt according to

$$A(T) = A_{1,2} (1 + A.T [(TL/300)^{M.AT-1}])$$

and

$$B(T) = B_{1,2} (1 + B.T [(TL/300)^{M.BT-1}])$$

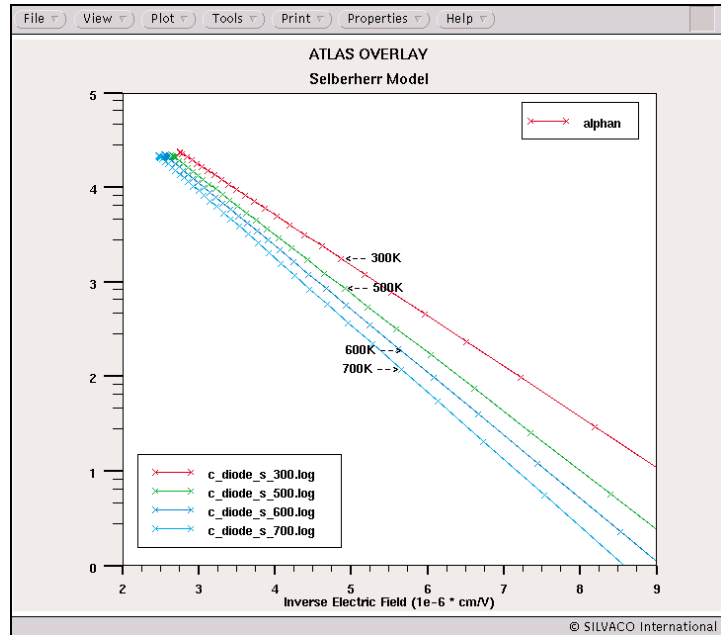


Figure 1. Variation of the electron ionization rate from Selberherr model, with inverse electric field for varying ambient temperatures.

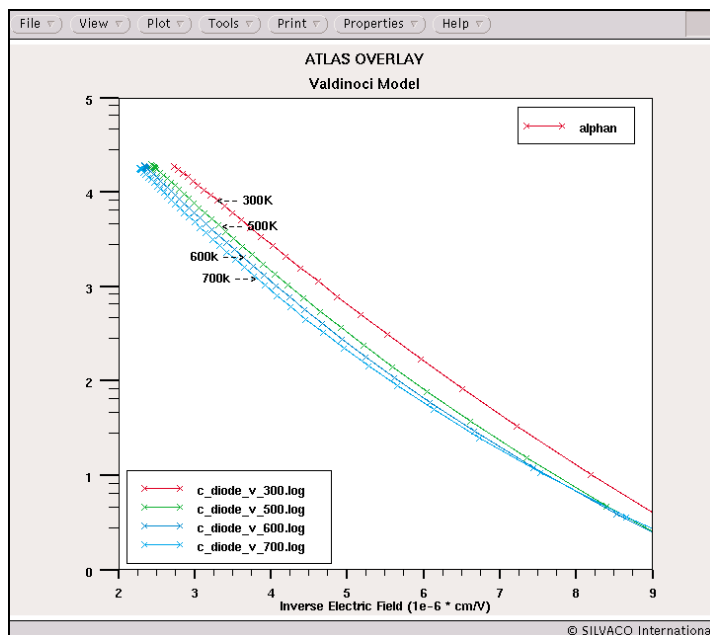


Figure 2. Variation of the electron rate from Valdinoci's model, with the inverse electric field for varying ambient temperatures.

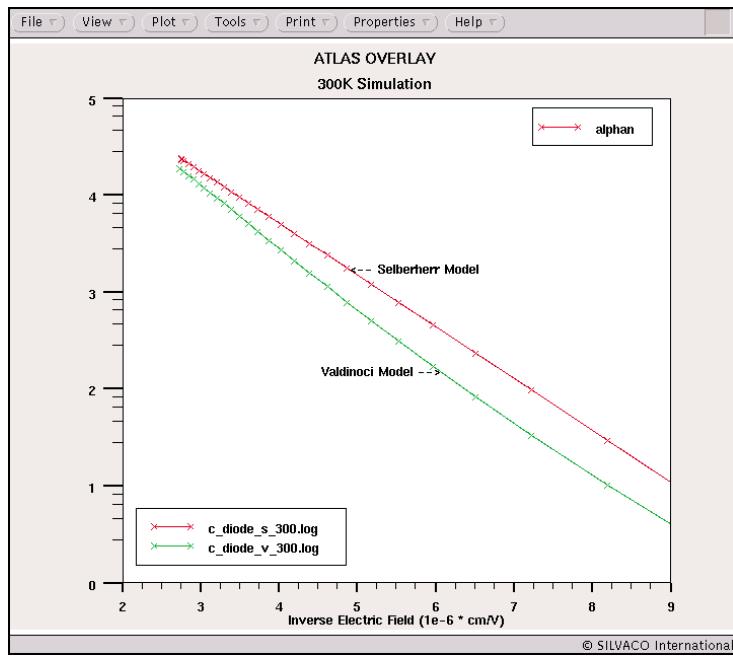


Figure 3. Comparison between the Valdinoci and Selberherr models of electron ionization rate at an ambient temperature of 300k.

Parameters	Electrons	Holes
a ₀	4-34	2.37
a ₁	-2.4x10 ⁻¹²	0.01
a ₂	4.12	1
b ₀	0.235	0.177
b ₁	0	-0.002
c ₀	1.68x10 ⁴	0
c ₁	4.38	0.09
c ₂	1	2.5
c ₃	0-13	0
d ₀	1.23x10 ⁶	1.4x10 ⁶
d ₁	1.2x10 ³	2.97x10 ³
d ₂	0.567	1.48

Table 1. Model parameter defaults.

A1 and B1 are used for $E < E_{GRAN}$; A2 and B2 are used for $E > E_{GRAN}$. (Note that the Valdinoci model reduces to the Selberherr model when its parameters are set to zero except for b₀ and d₀. But simpler is not necessarily more accurate.)

The electron or hole impact ionization coefficients at a location in a device can be recorded in a log file by specifying ALPHAN or ALPHAP in the PROBE statement. Figure 1 and Figure 2 each show a family of plots of electron ionization coefficient versus 1/E for the Selberherr model and the Valdinoci model. The Selberherr model gives straight lines (since beta=1 for silicon in this case) while the Valdinoci model shows a more complicated behavior. Figure 3 and Figure 4 compare the Selberherr and Valdinoci models directly at 300K and 700K. At 300K, both models give similar results, but at 700K the Selberherr model will underestimate low field impact ionization effects. In summary, the Valdinoci model is recommended for silicon devices which experience an extended temperature range of operation.

References

- 1) M. Valdinoci, D. Ventura, M. C. Vecchi, M. Rudan, G. Baccarani, F. Illien, A. Stricker, L. Zullino, "Impact-ionization in silicon at large operating temperature", SISPAD '99, Sept. 6-8, 1999, Kyoto, Japan.

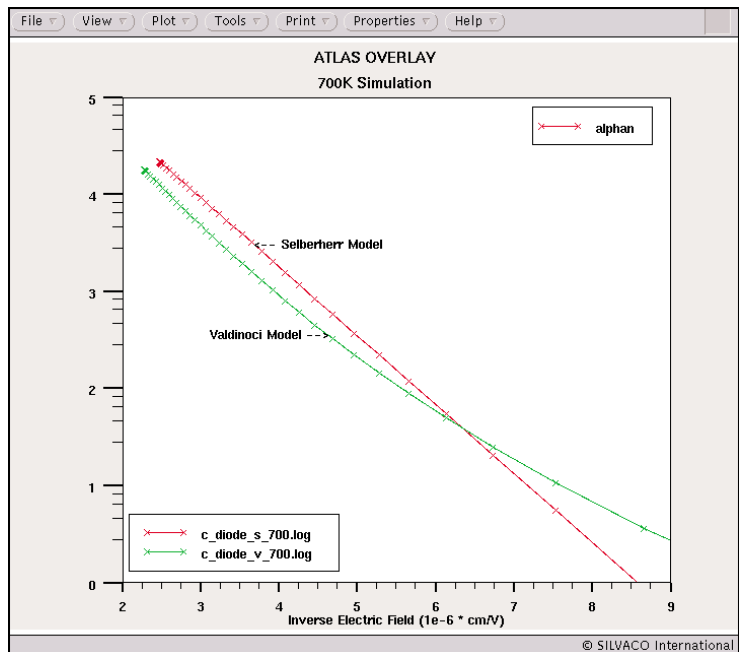


Figure 4. Comparison between the Valdinoci and Selberherr model of electron ionization rate at an ambient temperature of 700k.

Calendar of Events

August

1
2
3
4
5
6
7
8
9
10
11
12
13
14
15
16
17
18
19
20
21
22
23
24
25
26
27
28
29
30
31

September

1
2
3
4
5
6 <i>SISPAD 2002 - Osaka, Japan</i>
7
8
9
10
11
12
13
14
15
16
17
18
19 <i>RADECS - Padova, Italy</i>
20 <i>RADECS - Padova, Italy</i>
21
22 <i>IIT2002 - Taos, New Mexico</i>
23 <i>IIT2002 - Taos, New Mexico</i>
24 <i>IIT2002 - Taos, New Mexico</i> <i>ESSDERC - Florence, Italy</i>
25 <i>IIT2002 - Taos, New Mexico</i> <i>ESSDERC - Florence, Italy</i> <i>NUSOD - Zurich, Switzerland</i>
26 <i>IIT2002 - Taos, New Mexico</i> <i>ESSDERC - Florence, Italy</i> <i>NUSOD - Zurich, Switzerland</i>
27 <i>IIT2002 - Taos, New Mexico</i> <i>NUSOD - Zurich, Switzerland</i>
28
29 <i>BCTM - Monterey, CA</i>
30 <i>BCTM - Monterey, CA</i>

Bulletin Board



Workshop Schedule - Fall 2002 Scottsdale, Arizona

This fall, in addition to workshops with pre-scheduled topics, the Arizona Silvaco office will host two "open houses". These are times when Silvaco application engineers, computers, and software will be available to work with users to learn about new programs or features, or work on specific problems that users may be having. Attendance will be by registration, and space may be limited so we encourage you to sign up as soon as possible. These will be held at the Silvaco Office in Scottsdale. We may offer this at other locations if there is sufficient interest. Please let us know if you are interested in hosting a regional open house. Of course you are always welcome to visit Silvaco offices for demonstrations or support at other times - just contact your local office to set up an appointment.



On The Road in September

Silvaco will be showcasing its extensive suite of TCAD tools this September through a robust global trade show schedule. We will be discussing Radiation Effects on Components and Systems in Italy at this years RADECS show. Also in Italy you can come see us at the European Solid-State Device Research Conference. Rounding off our European tour we will be attending the Numerical Simulation of Semiconductor Optoelectronic Devices show in Zurich, Switzerland. Then over to Japan we can be found at the Solid State Device and Materials Conference in Tokyo. In the States we will be in New Mexico for the Ion Implantation Technology show and in Monterey, California for the BiPolar show (BCTM.) For information regarding any of the shows mentioned in this article please visit Silvaco.com.

If you would like more information or to register for one of our our workshops, please check our web site at <http://www.silvaco.com>

The Simulation Standard, circulation 18,000 Vol. 12, No. 8, August 2002 is copyrighted by Silvaco International. If you, or someone you know wants a subscription to this free publication, please call (408) 567-1000 (USA), (44) (1483) 401-800 (UK), (81)(45) 820-3000 (Japan), or your nearest Silvaco distributor.

Simulation Standard, TCAD Driven CAD, Virtual Wafer Fab, Analog Alliance, Legacy, ATHENA, ATLAS, MERCURY, VICTORY, VYPER, ANALOG EXPRESS, RESILIENCE, DISCOVERY, CELEBRITY, Manufacturing Tools, Automation Tools, Interactive Tools, TonyPlot, TonyPlot3D, DeckBuild, DevEdit, DevEdit3D, Interpreter, ATHENA Interpreter, ATLAS Interpreter, Circuit Optimizer, MaskViews, PSTATS, SSuprem3, SSuprem4, Elite, Optolith, Flash, Silicides, MC Depo/Etch, MC Implant, S-Pisces, Blaze/Blaze3D, Device3D, TFT2D/3D, Ferro, SiGe, SiC, Laser, VCSELS, Quantum2D/3D, Luminous2D/3D, Giga2D/3D, MixedMode2D/3D, FastBlaze, FastLargeSignal, FastMixedMode, FastGiga, FastNoise, Mocasim, Spirit, Beacon, Frontier, Clarity, Zenith, Vision, Radiant, TwinSim, , UTMOST, UTMOST II, UTMOST III, UTMOST IV, PROMOST, SPAYN, UTMOST IV Measure, UTMOST IV Fit, UTMOST IV Spice Modeling, SmartStats, SDDL, SmartSpice, FastSpice, Twister, Blast, MixSim, SmartLib, TestChip, Promost-Rel, RelStats, RelLib, Harm, Ranger, Ranger3D Nomad, QUEST, EXACT, CLEVER, STELLAR, HIPEX-net, HIPEX-r, HIPEX-c, HIPEX-rc, HIPEX-crc, EM, Power, IR, SI, Timing, SN, Clock, Scholar, Expert, Savage, Scout, Dragon, Maverick, Guardian, Envoy, LISA, ExpertViews and SFLM are trademarks of Silvaco International.

Hints, Tips and Solutions

William French, Applications and Support Manager

Q. Can ATLAS reproduce basic experiments to study the transient decay of carriers ?

A. Yes, ATLAS may be used to study these effects. A standard experiment for studying recombination in silicon is the transient decay of photoexcited carriers - known as the Stephenson-Keyes method for measuring minority carrier lifetime [1]. This method has been well described in [2]. The following is a description of the implementation of this experiment using the 2D device simulator ATLAS.

In the original experiment a constant current is passed through a n-type sample and a series of light pulses are shone onto the surface. The photogeneration causes a momentary increase in the conductivity which is observed as a voltage drop across the sample. This can be seen on an oscilloscope and used as a measure for lifetime. In this simulation a simpler method is possible. Under zero bias conditions a transient can be performed where the illumination is initially at 1 W/cm^2 . At a given time the illumination is suddenly turned off and the transient is continued out to a large time value, 1 ms.

Two observations should be apparent; first the minority carrier density under illumination should be

$$\text{hole density} = \tau_{\text{photo}} * G_{\text{photo}}$$

where G_{photo} is the photogeneration rate due to the light source and τ_{photo} is the minority (hole) carrier lifetime.

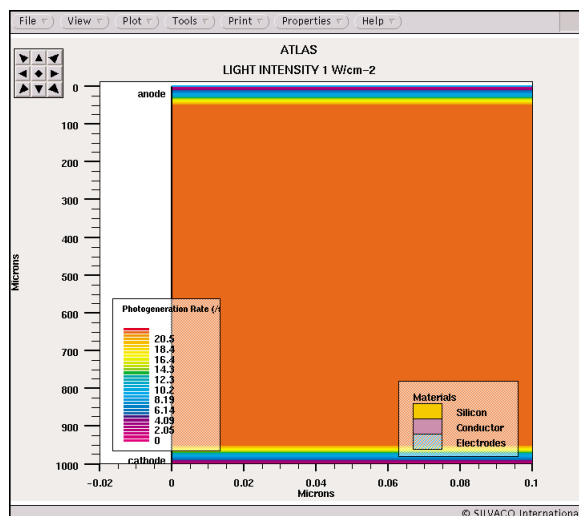


Figure 2. Two-dimensional structure under analysis. The light beam is switched on and photogeneration is plotted on the structure.

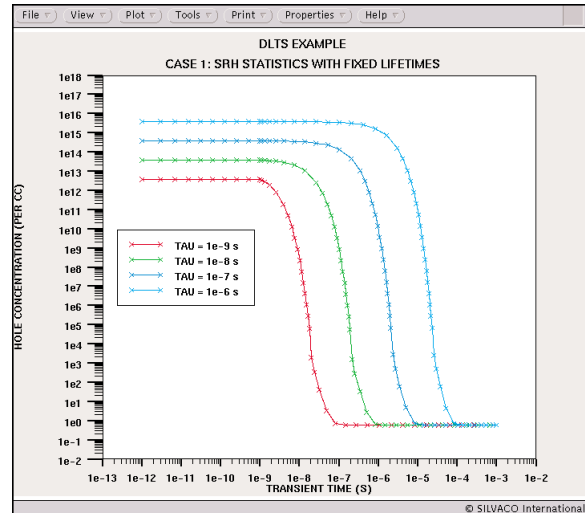


Figure 1. Transient simulation of hole current density for varying fixed carrier lifetimes. The Shockley-Read-Hall model was used for carrier recombination. The light intensity was 1 W/cm^2 and switched off at time $t=1e-9$ sec.

Second, when the light is switched off the minority carrier density should begin to fall off at a time equal to the carrier lifetime. It should decrease by a factor $1/e$ at that point. The simulated minority carrier density at a point in the structure can be saved during the transient analysis using the PROBE statement of ATLAS. This makes it straightforward to extract the carrier lifetimes.

Device Creation

An n-type silicon sample is created, using ATLAS/Spisces, with a heavy doping of $1e20 \text{ cm}^{-3}$ n-type. The heavy doping concentration is there to ensure that the device operates only under low injection conditions ie the excess minority carrier concentration, created by photogeneration, is much less than the majority carrier density. This is in accordance with the original experimental proposal. The device structure is also made to be very tall, 1000 um, so that any effects due to recombination at the contacts or on the surface do not interfere with the measurement of the bulk lifetime.

The silicon sample is defined to be sufficiently thin, 0.1 um in this case, so as to operate similar to a one-dimensional device. As a result the photogeneration rate is not susceptible to spatial decay and the photogeneration rate is then uniform across the sample.

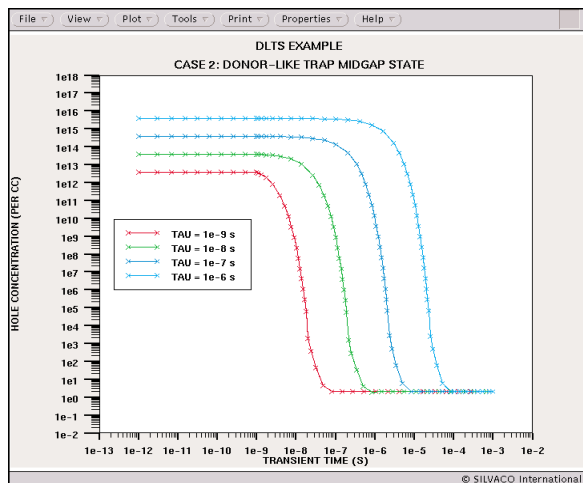


Figure 3. Transient simulation of hole current density. A donor-like trap was inserted into the bandgap and the carrier recombination calculated accordingly. The light intensity was 1 W/cm² and switched off at time t=1e-9 sec.

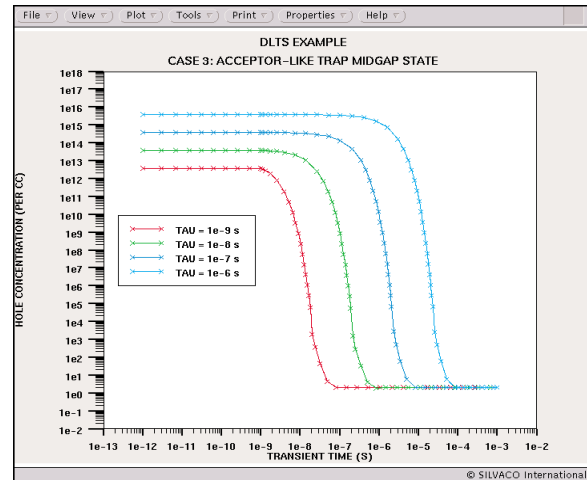


Figure 4. Transient simulation of hole current density. An acceptor-like trap was inserted into the bandgap and the carrier recombination calculated accordingly. The light intensity was 1 W/cm² and switched off at time t=1e-9 sec.

Physical Models

Two fundamental models may be used to simulate carrier recombination statistics in silicon. The first is the standard Shockley-Read-Hall recombination model where the simulation is defined with constant electron and hole recombination lifetime values. The second is to simulate the presence of mid-gap states explicitly as either donor or acceptor states.

Fermi statistics have been used in this analysis to remove any effects due to the high doping concentrations used.

Finally, the carrier mobilities were made artificially low, again to ensure that no contact effects are present.

Simulation Results

The first simulation has invoked the standard Shockley-Read-Hall statistics for carrier recombination. Four transient simulations were performed using fixed carrier lifetimes of 1e-6, 1e-7, 1e-8 and 1e-9 sec. Figure 1 shows the results of the phototransient on the minority (hole) density for these lifetimes. The light source is on until 1e-9 sec where it is turned off.

When the light beam is on there should be constant photogeneration through the structure and hence a constant hole density. Figure 2 shows the photogeneration rate in the structure for the case of a 1e-9 s carrier lifetime. Apart from directly underneath the contacts, a uniform photogeneration rate of approx 4e21 /scm³ is observed. The hole density should therefore be 4e21 * 1e-9 = 4e12 cm³ which is as shown in Figure 1.

To extract the lifetime from these plots is most easily done on a linear - linear scale and by extrapolating the minimum slope of the hole concentration to find the x-intercept on the time axis. This was performed using

an EXTRACT statement with the results as shown below for a lifetime of 1e-9 sec.

```
EXTRACT> extract name="Calc. Lifetime(1e-9) = "
(xintercept (minslope (curve (abs (time) , abs (probe.
" h+ conc. (per cc) ")))) - $"StartTime")
Calc. Lifetime(1e-9) = 1.05045e-09
```

The extracted lifetime (1.05045e-09 s) compared well with the simulated lifetime (1e-9 s).

Clearly the experimental extraction technique for minority carrier lifetime has been proved correct by the simulation.

The above simulation has been repeated with mid-gap states specified in the simulation. Figure 3 shows results for a donor-like trap situated 0.504 eV above the valence band. The lifetime associated with the trap was then varied as before. Figure 4 shows results for an acceptor-like trap situated 0.504 eV below the conduction band. The lifetime associated with the trap was then varied as before.

References

- [1] D.T. Stevenson and R.J. Keyes, "Measurement of Carrier Lifetime in Germanium and Silicon", J. Appl. Phys., 26, 190 (1955).
- [2] S.M. Sze, "Physics of Semiconductor Devices", Wiley, 1981, pp. 52-57.

Call for Questions

If you have hints, tips, solutions or questions to contribute, please contact our Applications and Support Department
 Phone: (408) 567-1000 Fax: (408) 496-6080
 e-mail: support@silvaco.com

Hints, Tips and Solutions Archive

Check out our Web Page to see more details of this example plus an archive of previous Hints, Tips, and Solutions
www.silvaco.com

Your Investment in Silvaco is SOLID as a Rock!!

While others faltered, Silvaco stood SOLID for 15 years. Silvaco is NOT for sale and will remain fiercely independent. Don't lose sleep, as your investment and partnership with Silvaco will only grow.

SILVACO INTERNATIONAL

USA HEADQUARTERS

Silvaco International
4701 Patrick Henry Drive
Building 2
Santa Clara, CA 95054
USA

Phone: 408-567-1000
Fax: 408-496-6080

sales@silvaco.com
www.silvaco.com

CONTACTS:

Silvaco Japan
jpsales@silvaco.com

Silvaco Korea
krsales@silvaco.com

Silvaco Taiwan
twsales@silvaco.com

Silvaco Singapore
sgsales@silvaco.com

Silvaco UK
uksales@silvaco.com

Silvaco France
frsales@silvaco.com

Silvaco Germany
desales@silvaco.com

*Products Licensed through Silvaco or e*ECAD*

